Vol. 31 (2000) *ACTA PHYSICA POLONICA B* No 3

A STUDY FOR THE NUCLEUS-NUCLEUS DIFFERENTIAL CROSS-SECTION

Z. Metawei

Physics Department, Faculty of Science, Cairo University
Giza, Egypt

(Received July 15, 1999; revised version received September 27 1999)

The near-side and the far-side decomposition following Fuller formalism have been calculated for the interaction of ^{12}C–^{12}C system at energies 1016, 1449 and 2400 MeV and for ^{16}O–^{12}C system at energy 1503 MeV. Fraunhofer oscillations observed at forward angles in the total differential cross-section are due to the strong interference between the near-side and the far-side contributions. The exponential fall off following the interference pattern is due to the dominance at large angles of the far-side amplitude and should thus be referred to as a far-side tail rather than a nuclear rainbow effect.

PACS numbers: 24.10.Cn

1. Introduction

It has been [1] observed that the differential cross-section measured at sufficiently high energies and at sufficiently large scattering angles when plotted as a ratio to Rutherford cross-section exhibits a characteristic monotonic, almost exponential falloff pattern at angles beyond those characterized by diffraction oscillations. This exponentiallike falloff is a characteristic of the nuclear rainbow [2] but not in and of itself definitive evidence of rainbow scattering. The scattering will then be characterized by a maximum deflection angle Θ, which will decrease with increasing bombarding energy. For fixed bombarding energies, Θ increases with increasing A.

Many authors [3–5] have suggested the discovery of nuclear rainbows in ^{12}C–^{12}C elastic angular distributions at various energies.

To study qualitative features of elastic scattering in the presence of strong absorption, the scattering amplitude is decomposed into what the semiclassical approach calls positive and negative deflection angle contributions [6]. For an amplitude obtained from partial wave summation, the decomposition of the scattering amplitude into positive and negative deflection angle contribution is done by considering the two amplitudes corresponding to the decomposition of each Legendre Polynomial into its two traveling wave components [6]. Fuller [6] has concluded that the smooth fall in tandem heavy ion elastic angular distributions arises from a diffractive shadow and not refractive or Coulomb rainbow shadow.

The refractive effects on scattering in the presence of strong absorption have been discussed by McVoy and Satchler [7] and they have concluded that a residuum of a true nuclear rainbow has been seen only for light ions. Such a rainbow seems to be unlikely for heavy ions because of their stronger absorption. For light heavy ion systems such as $^{12}C+^{12}C$, $^{16}O+^{12}C$ and $^{16}O+^{16}O$, it has been established that [7] the cross-sections are dominated by far-side scattering [7]. In particular there is often the appearance of a prominent (but damped) rainbow [7]. The angular distributions for elastic ^{12}C–^{12}C scattering at bombarding energies between 70 and 127 MeV have been presented together with the optical potential fit [8]. It has been found that at each energy, the far-sides of the optical potential scattering amplitude exhibit two or more Airy minima, which move forward in angle as the bombarding energy is increased [8]. The rainbows result from the interference of the inner and outer components of the far-side amplitude. It is pointed out that three conditions must be satisfied in the theoretical model and experimental data to fit the strong-interaction collision data [9], like $^{12}C+^{12}C$ and $^{16}O+^{16}O$ at laboratory energies below about 100 MeV/nucleon. These three conditions are:

(1) The real part of their interaction is strong enough ($V_0 \sim 200$ MeV) to produce far-side or nuclear rainbow oscillations in their elastic amplitudes, at certain characteristic bombarding energies [8,9].

(2) The imaginary part of this same interaction is weak enough ($W_0 \leq 30$ MeV) that these non-Fraunhofer oscillations are not "damped out".

(3) The data available extend to angles well beyond the Fraunhofer cross-over region, where the Airy or rainbow oscillations produced by this interference can be seen unsullied by the higher frequency Fraunhofer oscillations. This generally requires the measurement of very small cross-sections [9].

In a previous publication [10], the elastic scattering differential cross-section has been calculated for ^{12}C–^{12}C system at energy 1016 MeV and for ^{16}O–^{12}C system at energy 1503 MeV. These calculations were calculated including Pauli correlation effect. The depth of the real potential was $V_0 \sim 200$ MeV and the depth of the imaginary potential was $100 < W_0 < 200$ MeV.

We can see that our results for the real potential agree with the three conditions listed above, but the condition proposed for the imaginary potential is not satisfied. These calculations were improved by considering the target as deformed nucleus. In this work these calculations are extended to include the elastic scattering differential cross-section for ^{12}C–^{12}C system at energies 1449 and 2400 MeV. The scattering amplitude has been decomposed into its near-side and far-side components. It is found that the oscillations observed at forward angles in the total differential cross-section are due to the strong interference between the near-side and the far-side contributions. The exponential fall off following the interference pattern is due to the dominance at large angles of the far-side amplitude and should thus be referred to as a far-side tail rather than a nuclear rainbow effect. We have calculated the deflečtion function and the S-matrix. The formalism is presented in Section 2, Section 3 is devoted to the results and discussion. The conclusion is presented in Section 4.

2. The formalism

The elastic scattering differential cross-section for a symmetric system is given by

$$\sigma_{\rm el}(\theta) = |f(\theta) + f(\pi - \theta)|^2 , \tag{2.1}$$

while for non-symmetric system is given by

$$\sigma_{\rm el}(\theta) = |f(\theta)|^2 . \tag{2.2}$$

The elastic scattering amplitude considering the Coulomb effect is given by

$$f(\theta) = f_c(\theta) + (2ik)^{-1} \sum_{\ell} (2\ell + 1) \exp(2i\eta_\ell)(S_\ell - 1) P_\ell(\cos\theta) . \tag{2.3}$$

$f_c(\theta)$ is the usual point charge Coulomb amplitude, η_ℓ is the point charge Coulomb scattering phase shift, and S_ℓ is given by

$$S_\ell = \exp(2i\delta_\ell) , \tag{2.4}$$

where δ_ℓ is the complex nuclear phase shift, which is obtained from [11]

$$\delta_\ell = \frac{1}{2}\varkappa(b),$$

$$\varkappa(b) = \frac{-1}{2k} \int\limits_{-\infty}^{\infty} U(b,z) dz \tag{2.5}$$

with

$$U(b,z)=[2mA_PA_T(A_P+A_T)^{-1}]V_{\rm opt}(b,z)$$

k is the incident wave number and $V_{\rm opt}(b,z)$ is the optical potential.The nucleus-nucleus optical potential as derived by Wilson takes the form [12]

$$V_{\rm opt}(x)=A_PA_T\int d^3r_T\rho_T(r_T)\int d^3y\rho_P(x+y-r_T)t(e,y)[1-C(y)]\,, \quad (2.6)$$

where $A_i(i=P,T)$ are the mass numbers of the projectile and target, ρ_i are the ground state single particle nuclear densities for the colliding nuclei, $t(e,y)$ is the energy dependent constituent-averaged two nucleon transition amplitude obtained from scattering experiments, e is the NN kinetic energy in the c.m. frame, y is the NN relative separation and $C(y)$ is the Pauli correlation function, given by

$$C(y)\cong\frac{1}{4}\exp(-k_f^2y^2/10)\ \text{and}\ k_f=1.36\,{\rm fm}^{-1}\,. \quad (2.7)$$

$t(e,y)$ has been derived from the Fourier transform of the two body scattering amplitude [13]. We use the usual parametrization of the two body scattering amplitude:

$$f(e,q)=\frac{k_N\sigma}{4\pi}(\alpha+i)\exp(-Bq^2/2)\,. \quad (2.8)$$

This form of the scattering amplitude yields

$$t(e,y)=-\frac{e}{m}^{1/2}\sigma(\alpha+i)(2\pi B)^{-3/2}\exp\frac{-y^2}{2B}\,, \quad (2.9)$$

where q is the momentum transfer, k_N is the wave number of the incident nucleon, m is the nucleon mass, σ is the average nucleon-nucleon (NN) total cross-section, α is the average of the ratio of the real to the imaginary parts of the NN forward scattering amplitude and B is the slope parameter of the NN elastic scattering differential cross-section.

The near-side and far-side decomposition of the scattering amplitudes have been performed by replacing the associated Legendre polynomials $P_\ell(\cos\theta)$ by [6]

$$\widetilde{Q}_\ell^{\pm}(\cos\theta)=\frac{1}{2}\left[P_\ell(\cos\theta)\mp i\frac{2}{\pi}Q_\ell(\cos\theta)\right]\,, \quad (2.10)$$

where Q_ℓ is a Legendre function of the second kind.The recurrence formulas for P_ℓ and Q_ℓ are used in this equation. The far and near components of an amplitude obtained by partial wave summation are then given respectively by

$$f_F(\theta) = (2ik)^{-1} \sum_\ell (2\ell+1) \exp(2i\eta_\ell)(S_\ell - 1)\widetilde{Q}_\ell^+(\cos\theta)\,, \tag{2.11}$$

and

$$f_N(\theta) = (2ik)^{-1} \sum_\ell (2\ell+1) \exp(2i\eta_\ell)(S_\ell - 1)\widetilde{Q}_\ell^-(\cos\theta)\,. \tag{2.12}$$

The Rutherford scattering amplitudes for the near and the far sides are given by [6]

$$\frac{f_{R,N}(\theta)}{f_R(\theta)} = (1-e^{-2\pi\eta})^{-1} - \frac{i}{2\pi}\left[\sin^2\left(\frac{\theta}{2}\right)\right]^{1+i\eta} S(\theta) \tag{2.13}$$

$$\frac{f_{R,F}(\theta)}{f_R(\theta)} = -e^{-2\pi\eta}(1-e^{-2\pi\eta})^{-1} + \frac{i}{2\pi}\left[\sin^2\left(\frac{\theta}{2}\right)\right]^{1+i\eta} S(\theta)\,, \tag{2.14}$$

where

$$S(\theta) = \sum_{k\geq 0} \frac{(1+i\eta)_k}{k!}\left[\Psi(k+1) - \Psi(k+1+i\eta) - \ln\cos^2\left(\frac{\theta}{2}\right)\right]\cos^{2k}\left(\frac{\theta}{2}\right)\,.$$

3. Results and discussion

Near-side trajectories are the positive-angle ones (like Coulomb trajectories) corresponding to a repulsive interaction or reflection; Far-side trajectories are negative angle ones, passing behind the target, caused in general by a combination of diffraction and attractive interaction refraction [14]. The scattering amplitude can be written as a sum of near-side and far-side components

$$f(\theta) = f_N(\theta) + f_F(\theta) \tag{3.1}$$

whose most important property is that the Fraunhofer diffractive oscillations occur in neither f_N nor f_F but only in their interference; other types of interference, such as rainbow minima, occur in either f_N or f_F alone [14].

The contributions of the near-side and the far-side components to the elastic scattering cross-section have been calculated for the interactions of ^{12}C–^{12}C system at energy 2400 MeV. Fig. 1 shows the near-side and the far-side decomosition of the elastic scattering along with the total differential cross-section for the interactions of two spherical nuclei and the interactions of spherical projectile nucleus with deformed target nucleus. We can see

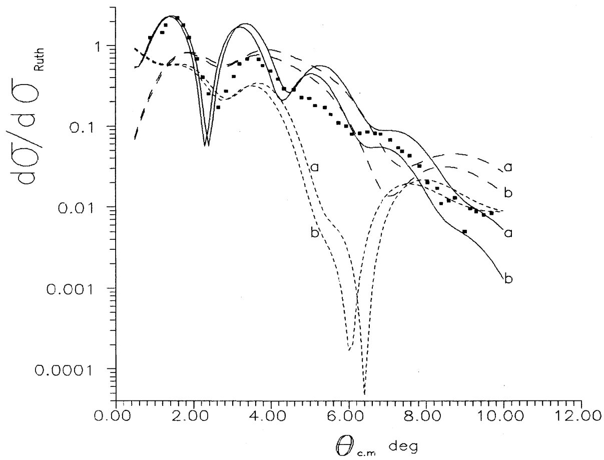

Fig. 1. The near-side (short dashed broken lines)and far-side (long dashed broken lines)decomposition of the elastic scattering differential cross-section are calculated for ^{12}C–^{12}C system at energy 2400 MeV. The elastic scattering differential cross-section is presented (solid line). These calculations are performed for: a — the interactions of two spherical nuclei and b — the interactions of spherical projectile nucleus with deformed target nucleus.

from Fig. 1 that considering the target as deformed nucleus improves the agreement of the total differential cross-section with the experimental data. The value of the near-side and the far-side components decreases by considering the target as deformed nucleus. At angle $\theta_{\rm c.m.} \geq 6$ the near-side cross-section calculated for two spherical nuclei decreases than that calculated for the interactions of spherical projectile with deformed target. Then, it increases again to have a larger value at $\theta_{\rm c.m.} \geq 8$. The behavior of the near-side and the far-side componants is not changed by considering the target as deformed nucleus. The crossover of the near-side and the far-side components occurs at the same point for the two cases considered. This shows that the modification of the Optical Model Potential by considering the target as deformed nucleus does not change the behavior of the near-side and the far-side components. We can see from Fig. 1 that the reactions are far-side dominated. The oscillations observed in the far-side distributions are due to the beating of the two waves belonging to the different negative branches of the deflection function. Also, we can see that the refractive contribution associated with the Coulomb rainbow is dominated at extreme forward angle, and its fall-off is steeper than that of the diffractive contribution. The oscillations in the near-side is caused by the interference of the refractive-diffractive decomposition of the near-side cross-section [15].

The contributions of the near-side and the far-side components to the elastic scattering cross-section have been calculated for the interactions of ^{12}C–^{12}C system at energies 1016,1449 and 2400 MeV and for the interactions of ^{16}O–^{12}C system at energy 1503 MeV. Fig. 2 shows the contributions of the near-side and the far-side components to the elastic scattering cross-section along with the total differential cross-section for the interactions of spherical projectile nucleus with deformed target nucleus. These calculations are compared with the experimental data [16–19]. Fig. 2(a) shows the contributions of the near-side and far-side components to the elastic scattering cross-section along with the total differential cross-section for the interactions of ^{12}C–^{12}C system at energy 1016 MeV. We can see from Fig. 2(a) that the oscillations observed at forward angles in the total differential cross-section are due to the strong interference between the near-side and the

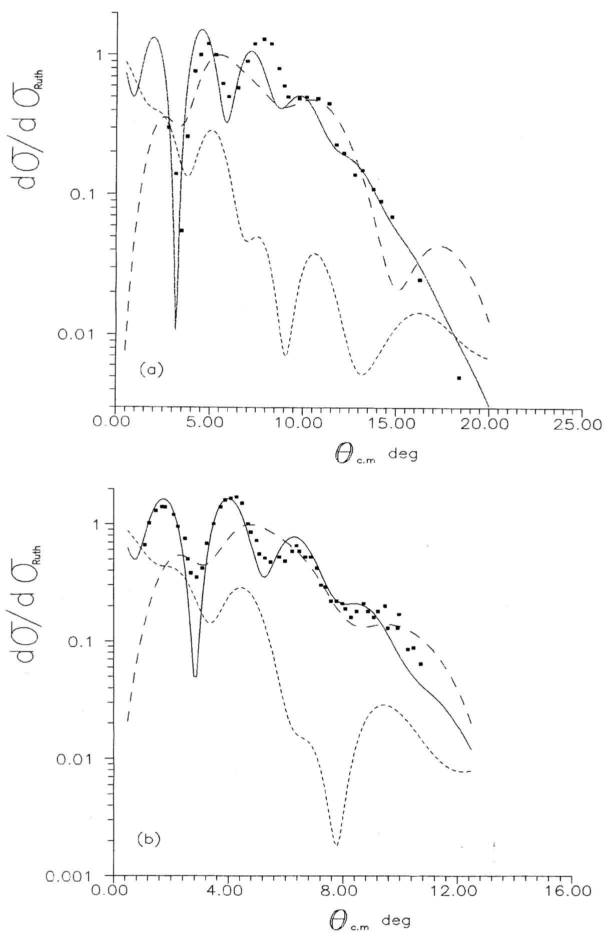

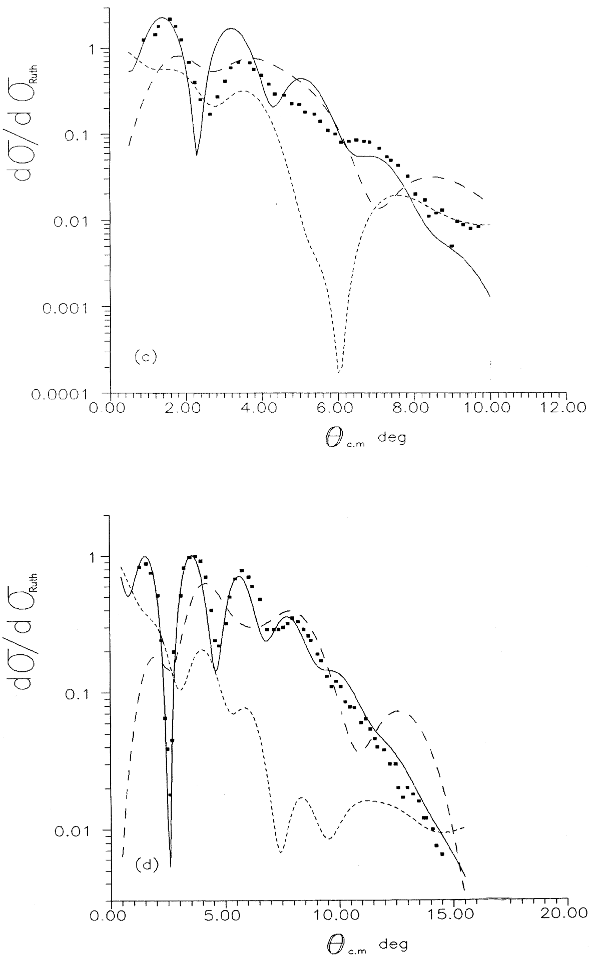

Fig. 2. The near-side (short dashed broken lines) and far-side (long dashed broken lines) decomposition of the elastic scattering differential cross-section are calculated for (a) ^{12}C–^{12}C system at energy 1016 MeV, (b) ^{12}C–^{12}C system at energy 1449 MeV, (c) ^{12}C–^{12}C system at energy 2400 MeV and (d) ^{16}O–^{12}C system at energy 1503 MeV. The elastic scattering differential cross-section is presented (solid lines). These calculations are performed for the interaction of spherical projectile nucleus with deformed target nucleus.

far-side contributions. The far-side and the near-side crossover occurs at angle $\theta_{\mathrm{c.m}} = 2.6°$. The minimum in the total differential cross-section is due to strong far-near destructive interference [6, 14]. The exponential fall off following the interference pattern is due to the dominance at large angles of the far-side amplitude and should thus be referred to as a far-side tail [16, 20] rather than a nuclear rainbow effect.

Concerning the interference between the near-side and the far-side components, Eq. (3.1) implies that the corresponding cross-section can be written as

$$|f(\theta)|^2 = |f_N(\theta)|^2 + |f_F(\theta)|^2 + 2\mathrm{Re}(f_N^*(\theta) f_F(\theta)) \,. \tag{3.2}$$

The term $2\mathrm{Re}(f_N^*(\theta) f_F(\theta))$ represents the interference between the near-side and the far-side scattering amplitudes. Fig. 3(a) shows the elastic scattering differential cross-section for the interactions of ^{12}C–^{12}C systems at energy 1016 MeV along with the interference of the near-side and the far-side scattering amplitudes for the same reactions. We can see from Fig. 3(a) that the positions of the minima and the maxima are the same for the elastic scatter-

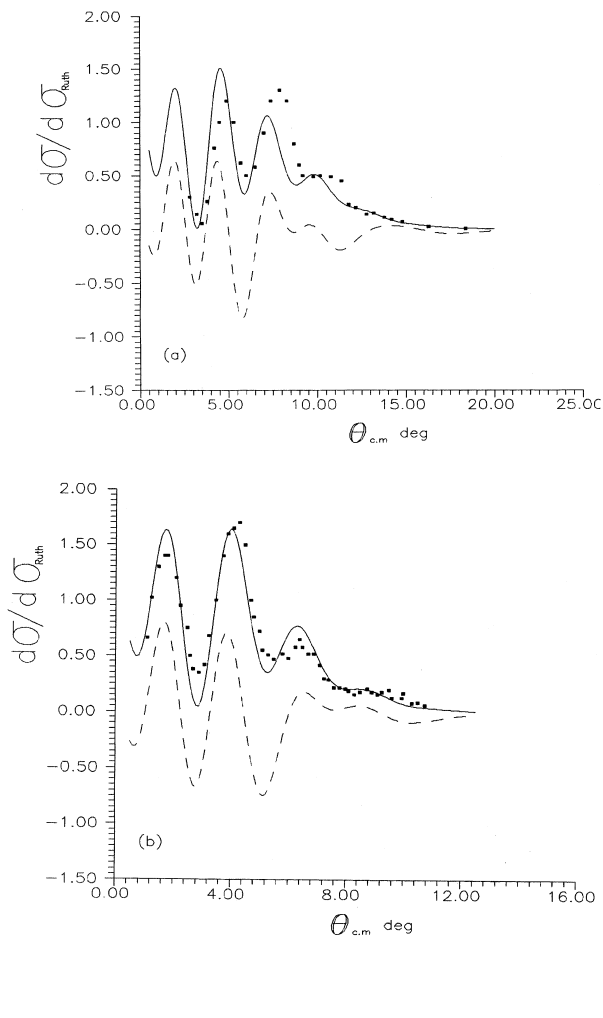

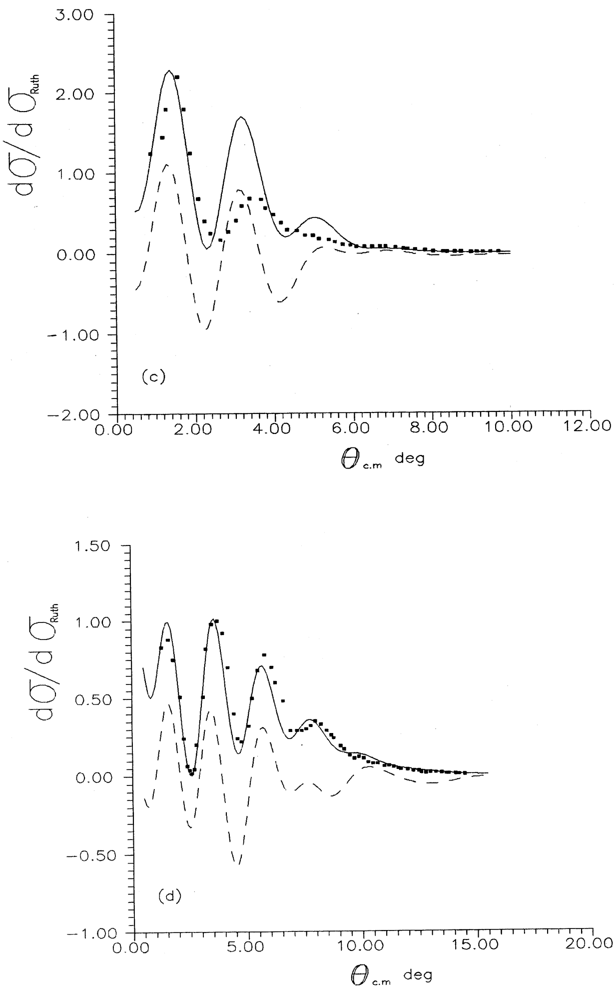

Fig. 3. The interference of the near-side and the far-side scattering amplitude(dashed line) are presented along with the elastic scattering differential cross-section (solid line) for (a) ^{12}C–^{12}C system at energy 1016 MeV, (b) ^{12}C–^{12}C system at energy 1449 MeV, (c) ^{12}C–^{12}C system at enegy 2400 MeV, (d) ^{16}O–^{12}C system at energy 1503 MeV. These calculations are performed for the interaction of spherical projectile nucleus with deformed target nucleus.

ing differential cross-section and the interference between the near-side and the far-side scattering amplitudes. This shows that the oscillations observed at forward angles in the total differential cross-section are due to the strong interference between the near-side and the far-side contributions.

It is seen from Fig. 2(a) that the far-side distribution shows oscillations. Oscillations will show up only if we have the beating of two waves belonging to the different negative branches of the deflection function [20].

The deflection function for the scattering by a real potential is

$$\Theta(\ell) = 2\frac{d\delta(\ell)}{d\ell}\,, \tag{3.3}$$

where $\delta(\ell)$is the total (coulomb + nuclear) phase shift. Fig. 4(a), (b) shows the deflection function for the reactions of ^{12}C–^{12}C system at 1016 MeV along with the S-matrix for the same reactions. The deflection function and the

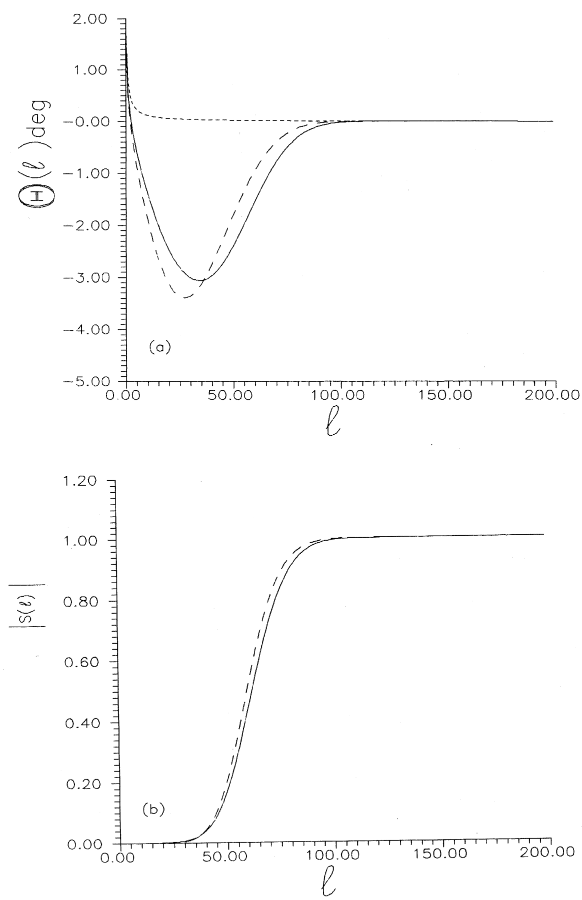

Fig. 4. Deflection function (a) and moduli of the S-matrix (b) for the interactions of ^{12}C–^{12}C system at energy 1016 MeV (solid lines). Long dashed broken line represent the calculations for two spherical nuclei. Short dashed line represents the deflection function for the Rutherford scattering.

S-matrix are calculated for two spherical nuclei and for spherical projectile with deformed target. We can see from Fig. 4(a) that the rainbow scattering angle value decreases by considering the target as deformed nucleus. The values of the nuclear rainbow angle θ_r, rainbow angular momentum L_r, grazing angular momentum L_g and the value of the modulus of S-matrix at the rainbow angular momentum $|S_{L_r}|$ are given in Table I and Table II. We can notice that the nuclear rainbow, minimum of the deflection function, is shifted toward the small S-matrix elements, lower L value than the grazing one. Our analysis indicates that $|S_L| \approx 0$ for $L < 29$, which show the strong absorption for smaller L values for the system of deformed target nucleus. We can notice that the residual rainbow feature has moved forward in angle that it overlaps with the far/near interference pattern. A result which is obtained by McVoy [7]. This shows that the nuclear rainbow obscured by the strong absorption [21]and cannot be recognized. The absorption for $L \leq L_r$ is strong enough to make a true rainbow pattern unobservable, but it is not strong enough to destroy the pattern of the far-side dominance due to the partial waves with L between L_r and L_g [7].

Fig.2(b) shows the near-side and the far-side contributions to the elastic scattering cross-section along with the total differential cross-section for the interactions of ^{12}C–^{12}C system at energy 1449 MeV. We can see from Fig. 2(b) that the Fraunhofer oscillation in the total cross-section is due to the interference between the near-side and the far-side components. A matter which is confirmed by calculating the interference term in eq.(3.2) together with the total cross-section as shown in Fig. 3(b). Fig. 3(b) shows that the distribution shape of the total cross-section is the same as that for the interference between the near-side and the far-side components. It is seen from Fig. 2(b) that the near/far crossover occurs at angle $\theta_{\text{c.m.}} = 1.8°$. The exponential fall off following the interference pattern is due to the dominance at large angles of the far-side amplitudes and should be referred to as a far-side tail rather than a nuclear rainbow effect. We can see from Fig. 2(b) also, that the far-side distribution shows oscillation pattern which is due to the beating of two waves belonging to the negative branches of the deflection function. The deflection function for the interaction of ^{12}C–^{12}C system at energy 1449 MeV is calculated along with the S-matrix for the same reaction. The calculations are performed for two spherical nuclei and for the interactions of spherical projectile with deformed target and the values of θ_r, L_r, L_g and $|S_{L_r}|$ are shown in Tables I and II. We can see from Table I and Table II that the nuclear rainbow is shifted toward the small S-matrix elements, lower L value than the grazing one. We have obtained also for deformed target nucleus that $|S_L| \approx 0$ for $L = 19$ which is a value smaller than that obtained for ^{12}C–^{12}C system at energy 1016 MeV. This shows that the absorption decreases with increasing the energy.

Fig. (2.c) shows the far-side and the near-side decomposition of the elastic scattering for ^{12}C–^{12}C system at energy 2400 MeV along with the total differential cross-section. We can see from Fig. 2(c) that the Fraunhofer oscillations in the total cross-section is due to the interference between the near-side and the far-side components,as we can see from Fig. 3(c). Fig. 3(c) shows a strong near/far interference. It is seen from Fig. 2(c) that the near/far crossover occurs at angle $\theta_{\mathrm{c.m.}} = 1.3°$. The exponential fall off following the interference pattern is due to the dominance at large angles of the far-side amplitudes and should be referred to as a far side tail rather than a nuclear rainbow effect. We can see from Fig. 2(c) that the far-side distribution shows oscillation pattern which is due to the beating of two waves belonging to the negative branches of the deflection function. The near-side distribution shows an oscillations and there are crossover between the near-side and the far-side at two points at large scattering angles. The oscillations in the near-side distribution are caused by the interference of the refractive and diffractive components of the near-side cross-section [15]. The deflection function and the S-matrix have been calculated for this reaction. The values of the rainbow angle θ_r, rainbow angular momentum L_r, grazing angular momentum L_g and the value of the modulus of S-matrix at the rainbow angular momentum $|S_{L_r}|$ are listed in Tables I and II. We can see from Tables I and II that the residual rainbow feature has moved forward in angle that it overlaps the far/near interference pattern. Also, the nuclear rainbow is shifted toward the small S-matrix elements, lower L value than the grazing one. We have observed that $|S_L| \approx 0$ for $L < 4$ from the calulations of the S-matrix for the interactions of spherical projectile with deformed target nucleus. This shows that the absorption for the lower partial waves becomes weaker than that for ^{12}C-^{12}C system at energies 1016 and 1449 MeV. So the beating of the two waves belonging to the different negative branches of the deflection function becomes stronger. The absorption is strong enough to make a true nuclear rainbow unobservable but it is not strong enough to destroy the pattern of the far-side dominance. We can see from Fig. 2(c) that the oscillations of the far-side amplitude becomes smoother than that obtained for ^{12}C–^{12}C reactions at energy 1016 and 1449 MeV.

Fig. 2(d) shows the near-side and the far-side distributions for the interactions of ^{16}O–^{12}C system at energy 1503 MeV, along with the total cross-section. Fraunhofer oscillation observed at the forward angles in the total cross-section is due to the near-side and the far-side strong interference as shown in Fig. 3(d). Fig. 3(d) shows the distribution of the near/far interference for the interactions of ^{16}O–^{12}C system at energy 1503 MeV along with the total cross-section. We can see from Fig. 3(d) that the distribution behavior of the near/far interference is the same as that for the total cross-

TABLE I

Parameter characterizing the deflection function and the S-matrix considering the target as deformed nucleus.

Reaction	Energy(MeV)	θ_r	L_r	L_g	$\lvert S_{L_r}\rvert$
^{12}C–^{12}C	1016	-3.06	34	62	0.01
^{12}C–^{12}C	1449	-1.89	41	70	0.05
^{12}C–^{12}C	2400	-1.26	52	88	0.07
^{16}O–^{12}C	1503	-3.25	41	80	0.01

TABLE II

Parameters characterizing the deflection function and the S-matrix for two spherical nuclei.

Reaction	Energy(MeV)	θ_r	L_r	L_g	$\lvert S_{L_r}\rvert$
^{12}C–^{12}C	1016	-3.39	27	60	0.002
^{12}C–^{12}C	1449	-2.21	32	68	0.01
^{12}C–^{12}C	2400	-1.40	42	85	0.02
^{16}O–^{12}C	1503	-3.62	34	78	0.001

section. We can see from Fig. 2(d) that the near/far cross-over occurs at angle $\theta_{\mathrm{c.m.}} = 2.7°$. The minimum in the total differential cross-section is due to strong far/near destructive interference. We can see also from Fig. 2(d) that the exponential fall off following the interference pattern is due to the dominance at large angles of the far-side amplitude and should thus be referred to as a far-side tail. The oscillations in the far-side distribution are due to constructive and destructive interference between the contributions from the two branches of the deflection function with $L > L_r$ and $L < L_r$. The deflection function has been calculated along with the S-matrix for the interaction of ^{16}O–^{12}C at energy 1503 MeV. These calculations are presented in Table I and Table II. We have observed that the absorption is strong for partial wave with $L < 39$. The absorption is strong enough to make a true nuclear rainbow unobservable but it is not strong enough to destroy the pattern of the far-side dominance. This is due to the partial waves with L between L_r and L_g. We can notice from Tables I and II that the nuclear rainbow angle is shifted toward smaller L values, also it is shifted toward smaller angle as we can see from Fig. 2(d), which show that it overlaps the interference between the near-side and the far-side components of the total cross-section. Also, the nuclear rainbow obscured by the strong absorption for $L < 39$.

We can see from Figs 2(a), (b), (c) that as the energy increases, the value of the differential cross-section decreases and the scattering angle decreases. Also, the values of the near-side and the far-side components decrease with increasing the energy. Comparing Table I and Table II, we can see that the rainbow scattering angle decreases by considering the target as deformed nucleus. However the values of the rainbow partial waves L_r and the grazing partial wave L_g increase by considering the target as deformed nucleus. Also, the values of the S-matrix at the rainbow partial wave increase by considering the target as deformed nucleus. We can see from Table I and Table II that the values of the rainbow angles decrease by increasing the energy. However the values of the rainbow partial waves , the grazing partial waves and the values of the S-matrix at the rainbow partial waves increase by increasing the energy. This shows that the behavior of θ_r, L_r, L_g and $|S_{L_r}|$ do not change by introducing the modification of considering the target as deformed nucleus to the Optical Model Potential.

4. Conclusion

The near-side and the far-side components of the elastic scattering have been calculated according to Fuller formalism for the interaction of ^{12}C–^{12}C system at energies 1016, 1449 and 2400 MeV and for ^{16}O–^{12}C system at energy 1503 MeV. It is found that there is a strong interference between the far-side and the near-side components of the elastic scattering. This strong interference is responsible about the Fraunhofer diffraction pattern observed in the elastic scattering distribution at the forward angles. It is found that the near/far crossover is shifted toward smaller angle as the energy of the system increased. The exponential fall off following the Fraunhofer diffraction pattern is due to the dominance at large angles of the far-side amplitude and should thus be referred to as a far-side tail [16, 20] rather than a nuclear rainbow effect. The oscillation observed in the far-side distribution is due to the beating of two waves belonging to the different negative branches of the deflection function [20]. The calculations of the deflection function show that the rainbow scattering angle value decreases with increasing the energy of the interaction. We also can conclude that the residual rainbow feature has moved forward in angle that it overlaps with the far/near interference pattern [7]. Calculating the S-matrix shows that the grazing partial wave L_g increases with increasing the energy and increases with increasing the mass of the projectile. The rainbow partial wave L_r corresponding to the rainbow angle θ_r increases with increasing the energy, however the absorption decreases with increasing the energy. Any residuum of the classical rainbow phenomenon would be exhibited in the far-side amplitude. One would expect an enhancement of the cross-section forward of the rainbow angle $\theta = \theta_r$. This characteristic has not been observed in our work or in the previous heavy ion scattering measurements [22]. Which show that the reflection of partial waves with $L \leq L_r$ is too weak $|S_L| \approx 0$ to produce observable effect. This means that the nuclear rainbow obscured by the strong absorption [21].

The author wishes to thank Prof. Dr. M.Y.M.Hassan, Head of Physics Department, Faculty of Science, Cairo University, for numerous fruitful discussions.

REFERENCES

[1] D.A. Goldberg, S.M. Smith, *Phys. Rev. Lett.* **29**, 500 (1972).

[2] D.A. Goldberg, S.M. Smith, *Phys. Rev. Lett.* **33**, 715 (1974).

[3] M.E. Brandan, *Phys. Rev. Lett.* **49**, 1132 (1982).

[4] H.E. Bohlen, M.R. Clover, G. Ingold, H. Letau, W. Von Oertzen, *Z. Phys.* **A308**, 121 (1982).

[5] M. Buenerd, *et.al.*, *Phys. Rev.* **C26**, 1299 (1982).

[6] R.C. Fuller, *Phys. Rev.* **C12**, 1561 (1975).

[7] K.W. McVoy, G.R. Satchler, *Nucl. Phys.* **A417**, 157 (1984).

[8] K.W. McVoy, M.E. Brandan, *Nucl. Phys.* **A542**, 295 (1992).

[9] M.E. Brandan, H. Chehime, K.W. McVoy, *Phys. Rev.* **C55**, 1353 (1997).

[10] M.Y.M. Hassan, Z. Metawei, *Acta Phys. Slovaca* **46**, 41 (1996).

[11] L.W. Townsend, H.B. Bidasaria, J.W. Wilson, *Can. J. Phys.* **61**, 867 (1983).

[12] J.W. Wilson, L.W. Townsend, *Can. J. Phys.* **59**, 1569 (1981).

[13] D. Slanina, H. McManus, *Nucl. Phys.* **A116**, 271 (1968).

[14] M.S. Hussein, K.W. McVoy, *Prog. Part. Nucl. Phys.* **12**, 103 (1984).

[15] M.R. Pato, M.S. Hussein, *Phys. Rep.* **189**, 129 (1990).

[16] M. Buenerd *et al.*, *Nucl. Phys.* **A424**, 313 (1984).

[17] J.Y. Hostachy *et al.*, *Phys. Lett.* **B184**, 139 (1987).

[18] S.M. Lenzi, A. Vitturi, F. Zardi, *Phys. Rev.* **C40**, 2114 (1989).

[19] P. Roussel *et al.*, *Phys. Rev. Lett.* **54**, 1779 (1985).

[20] M.C. Mermaz, *Z. Phys.* **A321**, 613 (1985).

[21] J. Chauvin, D. Lebrun, A. Lounis, M. Buenerd, *Phys. Rev.* **C28**, 28 (1983).

[22] G.R. Satchler, *et al.*, *Phys. Lett.* **128B**, 147 (1983).